Constraining curvature parameters via topology

B.F. Roukema[1,2] **and J.-P. Luminet**[3]

[1] Inter-University Centre for Astronomy and Astrophysics, Post Bag 4, Ganeshkhind, Pune, 411 007, India (boud@iucaa.ernet.in)
[2] Observatoire de Strasbourg, 11 rue de l'Université, F-67000 Strasbourg, France
[3] DARC, Observatoire de Paris-Meudon, 5 place Jules Janssen, F-92195 Meudon Cedex, France (Jean-Pierre.Luminet@obspm.fr)

Abstract. If the assumption that physical space has a trivial topology is dropped, then the Universe may be described by a multiply connected Friedmann-Lemaître model on a sub-horizon scale. Specific candidates for the multiply connected space manifold have already been suggested. How precisely would a significant detection of multiple topological images of a single object, or a region on the cosmic microwave background, (due to photons arriving at the observer by multiple paths which have crossed the Universe in different directions), constrain the values of the curvature parameters Ω_0 and λ_0?

The way that the constraints on Ω_0 and λ_0 depend on the redshifts of multiple topological images and on their radial and tangential separations is presented and calculated. The tangential separations give the tighter constraints: multiple topological images of known types of astrophysical objects at redshifts $z \lesssim 3$ would imply values of Ω_0 and λ_0 preciser than $\sim 1\%$ and $\sim 10\%$ respectively. Cosmic microwave background 'spots' identified with lower redshift objects by the Planck or MAP satellites would provide similar precision. This method is purely geometrical: no dynamical assumptions (such as the virial theorem) are required and the constraints are independent of the Hubble constant, H_0.

Key words: methods: observational – galaxies: quasars: general – galaxies: clusters: general – cosmology: distance scale – cosmology: theory – cosmology: observations

1. Introduction

Is the Universe 'open', flat or 'closed'? This is a major question in observational cosmology, where the meaning is generally intended to be, respectively: 'Is the curvature of the Universe negative, zero or positive?'

The latter question is quantified as the measurement of the density parameter, Ω_0, and the (dimensionless) cosmological constant, λ_0, which together determine the curvature $\kappa_0 \equiv \Omega_0 + \lambda_0 - 1$.[1] The value of κ_0 is negative, zero or positive for negative, zero or positive curvature respectively. Recent observations from faint galaxy counts, gravitational lensing, type Ia supernovae (Fukugita et al. 1990; Fort et al. 1997; Chiba & Yoshii 1997; Perlmutter et al. 1999) and from the cosmic microwave background (CMB) favour an approximately zero curvature, though what seems to be the presence of geodesic mixing in the COBE observations of the CMB would require a Universe which has negative curvature (Gurzadyan & Torres 1997).

However, if the words 'open' and 'closed' in the former question are interpreted to mean 'infinite' and 'finite' in spatial volume, respectively, and if the curvature is not positive, then answering the question requires knowing not only the curvature of the Universe but also its topology. In fact, the question should then be reworded into a double question: 'Is the Universe positively curved (hence finite)? If not, then is it infinite ("open") or finite ("closed") in volume?' A flat or negatively curved (hyperbolic) universe with a Friedmann-Lemaître-Robertson-Walker metric can be either infinite or finite, a common example of the latter being the flat hypertorus.

Moreover, measurement of the topology of the Universe is not only likely to be necessary to answer the question under the latter interpretation of the words 'open' and 'closed', but it would help to measure their quantitative meanings under the former interpretation as descriptions of curvature. The precision attainable is at least as good as that expected from the Planck and MAP satellites.

It is hoped that the global topology of the Universe can be either detected or shown in an assumption-free way to be non-measurable within the next decade. Several new observational methods to constrain, detect and/or measure the global topology of the Universe have been recently developed (Lehoucq et al. 1996; Roukema 1996; Cornish et al. 1996, 1998b; Roukema & Edge 1997; Uzan et al. 1999). The applications of these methods to observational programmes of major ground-based telescope and satellite projects already started or expected in the coming few years (SDSS, Loveday 1998; XMM, Arnaud 1996; Planck Surveyor; MAP) may well result in estimates of the topological parameters of the Universe, if these are measurable within the horizon defined in practice by the surface of last scattering (SLS).

Send offprint requests to: B.F. Roukema

[1] Note that Ω_0, λ_0 and κ_0 correspond to Ω, Ω_Λ and $-\Omega_R$ respectively in Peebles' (1993) notation.

Indeed, specific candidates for the 3-manifold of the spatial hypersurface projected to the present epoch have already been proposed (Roukema & Edge 1997; Bond et al. 1998).

It is therefore timely to examine how precisely a significant detection of multiple topological images of a single object or region on the CMB (due to photons arriving at the observer by multiple paths which cross the Universe in different directions) would constrain the values of Ω_0 and λ_0. This is the purpose of this paper.

Mathematically, the constraint on the curvature parameters is a consequence of the rigidity theorem of Mostow & Prasad (Mostow 1973; Prasad 1973), which constrains the curvature radius R_C (Eq. 2), and for a fixed value of R_C is a consequence of the effect that λ_0 has on the redshift-distance relation. To our knowledge, using topology to constrain curvature was first clearly mentioned in a cosmological context by Bernshtein & Shvartsman (1980).

1.1. The principle of constraining curvature parameters (Ω_0, λ_0) from multiple topological images

Cosmic topology is briefly described in Sect. 2.1.1.

In the case of a detection considered significant, photons emitted by a single collapsed object or from a single region of recombination epoch plasma would have crossed the whole Universe in different directions and probably more than once, before arriving at the observer in less than the age of the Universe. These would be considered to emanate from multiple topological images of a single object (or region).

The geometrical relationship between the apparent three-dimensional positions of the different topological images in the covering space (the naïve observer's space) is related to the shape of the fundamental polyhedron (parallelepiped in the case of the hypertorus). The linear transformations (isometries) between the multiple images, in the covering space, are integer linear combinations of the generators of a group of isometries. For the rectilinear hypertorus with no 'twists', the covering space is R^3, the topological images of a single object form a rectangular prismical lattice, the isometries are simply translations, and the generators are three mutually orthogonal vectors.

These isometries would hold for some particular values of Ω_0 and λ_0. If these curvature parameters are varied from the values for which the identification was discovered, then the distances between the identified images will no longer be related in the same proportions, and will no longer (in general) remain integer linear combinations of a set of generators. In other words, if the curvature parameters are varied, then the objects which previously had been identified as multiple topological images can no longer be explained as such.

Another way of looking at this is to consider the predictive power of candidate 3-manifolds. Given a candidate 3-manifold, the positions and redshifts of multiple topological images of all known objects visible to large redshifts can be predicted. If the candidate is correct, then observational confirmation of the predicted images will strengthen the hypothesis. However, if the candidate is correct in a limited redshift range to a certain pre-

cision, *but slightly wrong values for the curvature parameters are assumed,* then the multiple topological images in other redshift ranges will not occur at the predicted positions. The error will depend on the redshift and on the errors in the curvature parameters.

At low redshifts, the dependence of the metric on curvature is weak, so the constraints on Ω_0 and λ_0 would be weak. For multiple topological images at high redshifts distributed in the three-dimensional space inside of the SLS, the constraints would be much stronger, i.e. the uncertainties to within which Ω_0 and λ_0 could be estimated would be much smaller.

On the other hand, a detection of multiple topological imaging of circular subsets of the COBE maps (Cornish et al. 1998b), at the SLS, without confirmation from topological images inside of the SLS, would determine the sign of the curvature, and if this is non-zero, would fix the ratio R_H/R_C by the rigidity theorem, where R_H is the particle horizon radius[2] and R_C is the curvature radius [Eq. (2)].

Only a relation between Ω_0 and λ_0 would be known ($\Omega_0 + \lambda_0 = 1$ would be the relation for a 3-manifold with R^3 as the covering space), and extra information would be needed to find their individual values. This is because the SLS is essentially a spherically symmetric two-dimensional surface, i.e. a sphere, so that there is radial freedom in the relation between redshift and distance which would allow ranges of the values of the two curvature parameters which would leave the mappings on the sphere unchanged.

A CMB topology detection would, of course, be followed up by the search for sub-SLS topological images. If these were found at low redshifts $z \lesssim 0.5$, then the constraints on Ω_0 and λ_0 would most likely remain weak. If they were found at higher redshifts, $z \sim 3$, then the constraints would be stronger. However, the limited size of observational catalogues at higher redshifts, and the probable relative scarcity of astrophysically stable, bright objects at these redshifts, makes the latter a task much less straightforward than might be hoped for naïvely.

The goal of this paper is to estimate how precisely Ω_0 and λ_0 can be estimated, in practice, if sub-SLS multiple topological images are detected to high significance. The present value of the Hubble parameter, H_0, is only a scaling factor, so would not be constrained directly by topology detection. Conversely, the uncertainty of H_0 does not (to first order) affect the constraints on the curvature parameters by this method. However, independent constraints on $\Omega_0 h^{-2}$ or $\Omega_0 h$, such as from nucleosynthesis or from large scale structure, would provide good estimates of H_0 if Ω_0 were estimated to high precision (e.g. <1%).[3] Some comments regarding identification of objects in the CMB, e.g. cold spots, with their evolved, local counterparts are also made.

---

[2] Strictly speaking, what is constrained involves the distance to the SLS, which is slightly closer to us than the particle horizon that would be calculated if the matter-dominated regime is extended beyond the regime where it is physically correct. In order for the calculation to be mathematically correct, the difference between the two would have to be taken into account.

[3] The Hubble constant is parametrised as $h \equiv H_0/100 \text{ km s}^{-1} \text{ Mpc}^{-1}$.

1.2. Structure of paper and conventions

In Sect. 2, the reader is briefly reminded of some elements of the geometry of Friedmann-Lemaître universes (Sect. 2.1), and the method of deriving constraints on curvature parameters is explained (Sect. 2.2). The resulting precisions to which Ω_0 and λ_0 can be constrained are presented in Sect. 3. Discussion and conclusions are presented in Sect. 4 and Sect. 5.

Proper distances, in comoving coordinates, as in Eq. (1), are used throughout.

2. Method

2.1. The geometry of spatial sections ('space')

The application of general relativity to observations under the assumptions of a Friedmann-Lemaître universe results in three-dimensional spatial sections which may have non-zero curvature and/or non-trivial topology[4] (e.g. de Sitter 1917; Friedmann 1924; Lemaître 1958). Both possibilities were suggested in the pre-relativistic epoch by Schwarzschild (1900).

2.1.1. Cosmological topology

It is often implicitly hypothesized that the topology of the Universe is simply-connected. Since the density parameter is within an order of magnitude of unity, the observable sphere (inside the particle horizon) would in that case be much smaller than the Universe by a factor of 10^N where $N \gg 1$ [e.g. see Linde (1996) for discussion of inflation for zero versus negative curvature]. If this were correct, then observational cosmology would not be the study of the Universe, but only of a microscopic part of the Universe expected to be representative of the whole under some scenarios. This, of course, only provides an aesthetic criterion in favour of an observably 'small' Universe.

However, the requirement to have some sort of theory of quantum gravity at the Planck epoch ($t \sim 10^{-43}s$), and the fact that topological evolution in numerous dimensions is common in theories of particle physics, make a finite universe with a non-trivial topology (non trivial π_1 homotopy group) quite a theoretically likely possibility.

For general reviews on cosmological topology, see Lachièze-Rey & Luminet (1995); Luminet (1998); Starkman (1998); Luminet & Roukema (1999).

For theoretical work on physical explanations of the generation of topology at the quantum epoch, see recent articles such as Madore & Saeger (1997); Carlip (1998); Ionicioiu (1998); Dowker & Surya (1998); Dowker & Garcia (1998); Rosales (1998); e Costa & Fagundes (1998).

Recent observational methods of constraining and/or detecting candidates for the multiply connected manifold representing space include (i) cosmological microwave background (CMB), i.e. essentially two-dimensional methods (Stevens et al. 1993; Levin et al. 1998; Cornish et al. 1998b; Weeks 1998; Roukema 1999) and (ii) three-dimensional

analyses of the distribution of discrete cosmic objects, such as galaxy clusters and quasars (Fagundes & Wichoski 1987; Fagundes 1996; Roukema 1996; Lehoucq et al. 1996; Roukema & Edge 1997; Roukema & Blanloeil 1998; Lehoucq et al. 1999; Uzan et al. 1999). As mentioned above, some specific candidates for some or several of the generators defining the 3-manifold exist (Roukema & Edge 1997; Bond et al. 1998).

Several authors of the CMB methods have claimed lower limits to the size of the Universe of around 40% of the horizon diameter based on observational data from the COBE satellite, particularly for the case of zero curvature, but these claims remain controversial. Cornish et al. (1998a) argue that the resolution of COBE is insufficient for any constraints on topology, but more fundamentally, the problem is one of self-consistency of assumptions and hypothesis. Even though the hypothesis tested is that of a small universe, the assumptions made are those which are expected theoretically for a large universe, and which have only been observationally supported under the assumption of simple-connectedness.

If the Universe is observably multiply connected, then the standard version of inflation cannot quite be correct. Even if inflation is retained to solve various problems, it would be surprising to expect that it would have resulted in exactly gaussian perturbation statistics with a Harrison-Zel'dovich scale-free spectrum *on the scale of the fundamental domain*. Moreover, justifying the latter properties from a COBE data analysis under the assumption of simple-connectedness would not be valid. In fact, the articles claiming constraints from COBE data generally find that a small percentage of their perturbation simulations based on such assumptions are consistent with the COBE data, but do not examine what properties of the perturbations are required for small universe models and observations to be consistent.

Here, the reader is just reminded of a few aspects of cosmological topology. A simple two-dimensional analogy for a space (surface) with a non-trivial topology is the 2-torus, T^2, which can be imagined equivalently either as

(1) a torus placed in Euclidean 3-space, R^3, but given an *intrinsic* metric such that the curvature is zero everywhere on the surface; or as

(2) a rectangle whose opposite sides are identified; or as

(3) an infinite grid of multiple copies of a single rectangle corresponding to multiple copies of a single physical space.

Case (3) corresponds to what is termed the *'universal covering space'*, in this case R^2. A single copy of the rectangle, as in cases (1) or (2), is termed the 'fundamental domain', or 'Dirichlet domain', or in the three-dimensional case, the *'fundamental polyhedron'*. Mathematically, the 2-torus can be derived from R^2 by the isometric transformations which are simply translations in two perpendicular directions, i.e. $T^2 = R^2/\Gamma$, where Γ is the group generated by the two translations.

The corresponding three-dimensional space is the 3-torus, T^3, for which case (1) is difficult to imagine, case (2) involves identification of opposing faces of a rectangular prism, and case (3) has R^3 as the covering space.

---

[4] non trivial π_1 homotopy group

This is only one example. In general, the 3-manifolds of cosmological interest (i.e. with constant curvature) can be represented in terms of a fundamental polyhedron embedded in the appropriate covering space (H^3, R^3 or S^3 for negative, zero or positive curvature respectively), of which faces are identified in a certain way. The metric is that of the covering space. The isometries mapping one copy of the fundamental polyhedron to another within the covering space are linear (integer) combinations of the *generators* which form the holonomy group Γ.

If the fundamental polyhedron is 'smaller' than the SLS, then multiple topological images of astrophysical objects or of temperature fluctuations averaged over small regions of space should be visible. The smallest size of a (spatial) geodesic linking a point to itself (i.e. joining any two topological images of a single object) is labelled $2r_{\text{inj}}$, the *injectivity diameter*, while the diameter of the smallest sphere, in the covering space, which contains the fundamental polyhedron is termed $2r_+$, the *out-diameter*.

It is possible that $r_{\text{inj}} \ll r_+$. For hyperbolic (negative curvature) 3-manifolds, of which an infinite number are topologically distinct, it is common to have small values of r_{inj}. This means it would be possible to have many topological images in some directions of the observable sphere, but no topological imaging in other directions.

In the candidate hyperbolic manifold of Bond et al. (1998, Sect. 4.3), although the volume of the space is larger than that of the observable sphere, the injectivity diameter is slightly smaller, i.e. $r_{\text{inj}} \approx 0.96R_H$. That is, if population III globular cluster-like objects were visible just after recombination, then in some directions of the sky they would have topological images visible at certain positions on the CMB, assuming a future CMB satellite can reach the required resolution and sensitivity.

The candidate manifold of Roukema & Edge (1997) is more readily falsifiable: 965 ± 5 h^{-1} Mpc $< 2r_{\text{inj}} < 1190 \pm 10$ h^{-1} Mpc depending on the values of the curvature parameters. For a review of arguments for and against this candidate, see the discussion section of Roukema & Bajtlik (1999).

2.1.2. Curvature and distance-redshift relations

In the covering space, relations between the redshift and the proper distance (projected onto the present epoch, $t = t_0$), depend on the curvature parameters indicated above: Ω_0 and λ_0.

The proper distance to a redshift z is

$$d(z) = \frac{c}{H_0} \int_{1/(1+z)}^{1} \frac{da}{a\sqrt{\Omega_0/a - \kappa_0 + \lambda_0\, a^2}} \quad (1)$$

where $\kappa_0 \equiv \Omega_0 + \lambda_0 - 1$ as above. This is related to the curvature radius

$$R_C \equiv \frac{c}{H_0\sqrt{|\kappa_0|}} \quad (2)$$

and the proper motion distance $d_{\text{pm}}(z)$ by

$$d(z) = \begin{cases} R_C \sinh^{-1}[d_{\text{pm}}(z)/R_C], & \kappa_0 < 0 \\ d_{\text{pm}}(z), & \kappa_0 = 0 \\ R_C \sin^{-1}[d_{\text{pm}}(z)/R_C], & \kappa_0 > 0. \end{cases} \quad (3)$$

If $\Omega_0 > 0$ and $\lambda_0 = 0$, then

$$d_{\text{pm}}(z) = \frac{c}{H_0} \frac{2[z\Omega_0 + (\Omega_0 - 2)(\sqrt{\Omega_0 z + 1} - 1)]}{\Omega_0^2(1 + z)} \quad (4)$$

is a commonly used closed expression for the proper motion distance (Weinberg 1972, p.485). For non-zero values of λ_0, Eqs. (1), (2) and (3) provide an integral expression for d_{pm}. Values of these distances in physical units of typical astrophysical objects and of the particle horizon are shown in Fig. 1 of Roukema & Blanloeil (1998).

2.2. Uncertainties in Ω_0 and λ_0

An order of magnitude estimate of the uncertainty in the curvature parameters can be made as follows. For an object seen at $z \sim 3$, $\Delta z \sim 0.002$ corresponds to a precision of ~ 1h^{-1} Mpc. The proper distance to $z = 3$ ranges from 3000h^{-1} Mpc to ≈ 5000h^{-1} Mpc for $1 > \Omega_0 > 0.2$, $\lambda_0 \equiv 1 - \Omega_0$.

Then the difference in proper distance over the full range of curvature parameters is ≈ 2000h^{-1} Mpc, so that a precision of 1h^{-1} Mpc corresponds to 0.05%. If the dependence of proper distance on Ω_0 and λ_0 were roughly linear over this range, then for a fixed value of the proper distance to the object at $z = 3$, the uncertainties in Ω_0 and λ_0 would also be less than 0.1%. This is at least as precise as expected from the future CMB satellites Planck and MAP.

Of course, this is only an order of magnitude estimate, which doesn't take into consideration the actual numbers and relative geometry of multiple topological images. In reality, many topological images would have to be identified before a candidate manifold could be considered significant, and the accuracy of the values of the curvature parameters would be iteratively improved as more topological images are included in a best fit solution.

2.2.1. Separation into radial and tangential components

The objects whose three-dimensional positions are most sensitive to the curvature parameters are those at the highest redshifts. Both the radial and tangential components will be more sensitive at higher redshifts. If the curvature is negative, then due to the sinh factor the tangential components should be more sensitive than the radial components, and vice versa for positive curvature.

The separations at lower redshifts, which would be less sensitive to curvature parameters, could be considered as relatively fixed values for use at the higher redshifts.

To characterise these dependences, idealised cases of topological images separated in radial and tangential directions, shown in Fig. 1, are considered. These are only fictional constructs, particularly the latter, since the value of $2r_{\text{inj}}$ must be
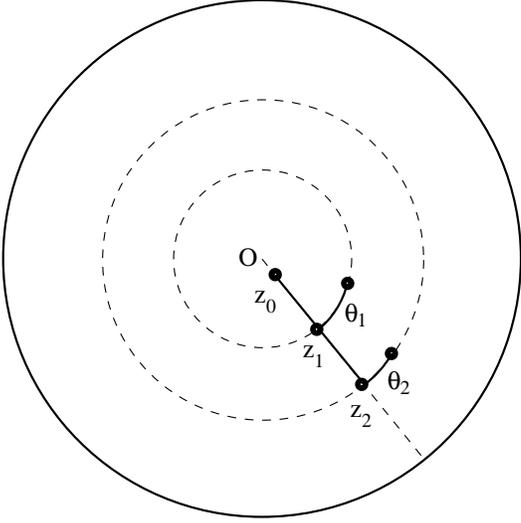
Fig. 1. Relative positions within the covering space of topological images used in the calculation, in spherical coordinates centred at the observer and limited by the surface of last scattering. For the radial component, three images are assumed to line up in an exactly radial direction, at redshifts z_0, z_1, z_2, covering two equal proper distance intervals, each of $2r_{inj}$. For the tangential component, a pair of images at z_1 separated along a circular arc by $2r_{inj}$ and another pair of images separated by $2r_{inj}$ along a circular arc at z_2 are considered. This latter is only a useful theoretical construct and would not (in general) occur in reality. If the curvature is zero, then the angles subtended at z_1 are related by $\theta_2/\theta_1 = d(z_1)/d(z_2)$, but for a non-zero curvature, additional sinh or sin factors are required. The proportions shown in the figure are correct if the distance to z_1 is one curvature radius, $\Omega_0 \approx 0.3$, $\lambda_0 \approx 0.0$ and $2r_{inj} \approx 3000h^{-1}$ Mpc.

a large fraction ($\gg 1\%$) of a horizon radius, so that $\theta_i \ll 1$ rad, $i = 1, 2$ is not valid, and the spatial geodesics joining the pairs of images at z_1 and z_2 (as opposed to the arcs joining them) will not be equal, except in special cases.

Small variations in the redshifts, due to spectroscopic uncertainty or to the inability to correct for peculiar velocities, then imply variations in Ω_0 and λ_0 needed in order to retain the equalities in the radial or tangential distances defining z_0, z_1, z_2, θ_1 and θ_2. The resulting quantities are $\partial\Omega_0/\partial z_i$ and $\partial\lambda_0/\partial z_i$, where $i = 0, 1, 2$ in the radial direction and $i = 1, 2$ in the tangential direction.

In a real case, the separations between topological images will not generally be either radial nor tangential, so the uncertainties will be somewhere in between these two limiting cases.

This is equivalent to inverting Eq. (1) so that the curvature parameters are functions of proper distance and redshift.

2.2.2. Cosmological redshift uncertainties

To determine the uncertainties in Ω_0 and λ_0, the derivatives $\partial\Omega_0/\partial z_i$ and $\partial\lambda_0/\partial z_i$ need to be combined with the uncertainty in the cosmological component of the redshift.

As pointed out in Sect. 2 of Roukema (1996), this uncertainty in the cosmological (smooth expansion) component of

the redshift can be separated into (1) the spectroscopic uncertainty,[5] (2) two components due to the peculiar velocity: (2a) movement of an object between two different epochs and (2b) the error caused by assuming the observed redshift to be purely cosmological. For physically reasonable values of the peculiar velocity and redshifts $z \lesssim 3$, the error (2a) is a small fraction of that due to (2b).

A typical precision practical for the spectroscopic uncertainty is $\Delta z \sim 0.001$ for an object such as a quasar, though much higher precision is possible. In that case the uncertainty is dominated by the peculiar velocity. A conservative upper limit to the peculiar velocity, assuming the quasar to be at the centre of a typical galaxy, can be taken as $\Delta(zc) \sim 600\,\mathrm{km\,s^{-1}}$, i.e. $\Delta z \sim 0.002$.

For a cluster of galaxies, spectroscopic redshifts could be found very precisely for individual galaxies, but a central velocity would have to be obtained from a fit to the distribution of the galaxies' velocities, assuming isotropy of the peculiar velocities within the cluster. The X-ray velocity of the peak of the X-ray distribution would provide another way to estimate the true cluster redshift, inclusive of the peculiar velocity of the cluster as a whole.

If two topological images of the cluster were at similar redshifts, as in the candidate identity suggested by Roukema & Edge (1997), then as pointed out by Roukema & Bajtlik (1999), transverse velocities could be measured for the galaxies in the cluster, and it would be possible to derive a detailed dynamical model implying an even preciser cluster velocity.

However, the peculiar velocity of the cluster as a whole would probably dominate the error. Here, $\Delta z \sim 0.002$ is adopted as a typical value.

For 'objects' such as cold spots in the CMB (Cayón & Smoot 1995), the uncertainty in the redshift would be related to the thickness of the SLS. The latter is $\Delta z \sim 100$ (and the SLS redshift is $z \sim 1100$; White et al. 1994; Bond 1996). This corresponds to a comoving thickness of ~ 10–$20h^{-1}$ Mpc.

2.2.3. Uncertainties in angles

Astrophysical objects at sub-horizon distances such as quasars and clusters of galaxies can have their angular positions measured much more precisely ($\sim 1''$ for quasars; a few arcseconds for clusters if gravitational lensing is available) than their cosmological redshifts. So, the error contributed to relative distance estimates is negligible relative to the error from redshift uncertainty.

If identification of COBE cold spots with local superclusters were successful, then the poor angular resolution of COBE ($\sim 10°$ FWHM) would introduce an uncertainty of $\sim 15\%$ in the tangential components at the redshift of the SLS, so the total

---

[5] Photometric redshifts presently attain a precision of ~ 0.1 (e.g. Miralles et al. 1999), but this is too imprecise for topological purposes.

.2   .6   .8   .10   .12

.4   .1   .3   .7   .9   .11
     ⊙

   .5
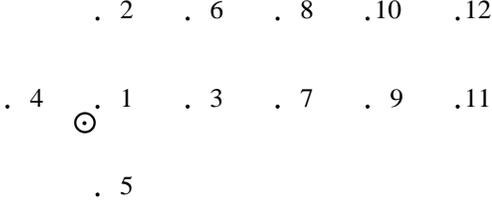
Fig. 2. Simulated order of observationally confirming positions of topological images of the hypothetically single cluster Coma/ RX J1347.5-1145/ CL 09104+4109. The three known clusters are numbered 1,2,3 respectively; following numbers indicate successive 'observations'. The Sun is indicated near the position of the Coma image.

uncertainties $\Delta\Omega_0$ and $\Delta\lambda_0$ would be much larger than just $\partial\Omega_0/\partial z_i \Delta z_i$ and $\partial\lambda_0/\partial z_i \Delta z_i$.

In contrast, Planck and MAP, with expected resolutions of $\sim 0.1°$ and $\sim 0.3°$ respectively, would provide good tangential constraints.

2.2.4. An illustrative simulation

The format according to which the first significant detections may be made is unpredictable, but to illustrate the way the radial and tangential uncertainties in the curvature parameters combine, a simulation is made in which it is hypothesized that cluster images are observed at the positions and redshifts predicted by the candidate 3-manifold of Roukema & Edge (1997).

According to this candidate 3-manifold, which can be called (with a slight abuse of language) a 2-torus, T^2, (though really it is $T^2 \times R$), the size of the Universe is $2r_{inj} \approx (965 \pm 5) h^{-1}$ Mpc for $\Omega = 1$ [$2r_{inj} \approx (1190 \pm 10) h^{-1}$ Mpc for $\Omega_0 = 0.2$, $\lambda_0 = 0.8$] in two nearly perpendicular directions, and in the third perpendicular direction the size is unknown, i.e. $r_+ > r_{inj}$. Photons approaching the observer from greater distances in these directions would have already crossed the Universe once or more, so the rich clusters RX J1347.5-1145 and CL 09104+4109 would be images of the Coma cluster seen about $2.8 h^{-1}$ Gyr ago for $\Omega = 1$ ($3.3 h^{-1}$ Gyr for $\Omega_0 = 0.2$, $\lambda_0 = 0.8$).

In the covering space, images of this cluster should form a nearly square lattice (grid) out to the redshift at which the cluster formed. For the simulation, it will be assumed that the first 'confirmations' of the hypothesis are detections of clusters at the 'antipodal' directions to RX J1347.5-1145 and CL 09104+4109, (the positions are antipodal from a Coma-centred viewpoint) and that successive confirmations of images are made first to successively higher redshifts, and then in roughly 'tangential' directions. This is, of course, an idealised simulation, ignoring systematic problems like foreground clusters or galaxies, dust, etc. This pattern of 'confirmation' is shown in Fig. 2.

The simulations are performed as follows. For a given choice of Ω_0 (λ_0 is constrained as $\lambda_0 = 1 - \Omega_0$ since the model is flat), $N = 100$ simulated sets $\{z_i\}_{i=4,i_{max}}$ are generated. The z_i values are calculated by assuming the generators to be exactly the vectors from Coma to RX J1347.5-1145 and CL 09104+4109, where spectroscopic and peculiar velocity errors are assumed to be zero for these three images, and by choosing a single

combined spectroscopic plus peculiar velocity error for each $i = 4, ..., i_{max}$ from a gaussian distribution centred at zero with dispersion $\sigma = 0.002$.

For a given simulation, the 'observational' deduction of the best fit Ω_0 value needs to be found. Over the N simulations, the distribution in the differences between input and output values of Ω_0 determines the uncertainty in the value of Ω_0.

The method of finding the 'best fit' value of Ω_0 for a given simulation is to find the value of Ω_0 for which the 'images' of the two generators are most self-consistent. That is, the value of Ω_0 is found which minimises

$$\begin{aligned} \sigma^2 &= \sigma_1^2 + \sigma_2^2 \\ &= \sum_i^{i_{max}} d_1(i,j)^2 + \sum_i^{i_{max}} d_2(i,j)^2 \end{aligned}$$

where the values of (i,j) used for distances d_1 are 4–1, 1–3, 2–6, 3–7, 6–8, 7–9, 8–10, 9–11 and 10–12 (up to the value of i_{max}) and those for d_2 are 1–2, 1–5, 3–6, 7–8, 9–10, 11–12 (up to the value of i_{max}). See Fig. 2 for the image numbering. This uses a close to maximal amount of nearly independent information, i.e. for what in principle are two spikes in the crystallographic method (Lehoucq et al. 1996), but a single spike in practice since the two generators are of equal lengths to within 1%.

3. Results

3.1. Radial and tangential components

The relations $\partial\Omega_0/\partial z_i$ and $\partial\lambda_0/\partial z_i$ have been calculated for values of the curvature parameters spanning the values of observational interest, and multiplied by $\Delta z = 0.002$ to give estimates of $\Delta\Omega_0$ and $\Delta\lambda_0$. These are shown in Figs 3 and 4.

As expected, the figures clearly show that

(i) the higher redshift objects provide preciser constraints than the low redshift objects
(ii) the tangential constraints are preciser than the radial ones
(iii) for sets of objects at redshifts $1 + z < 4$, a precision of better than 1% in Ω_0 and 10% in λ_0 is possible.

Any single set of three topological images separated in a *radial direction* would correspond to a combination of three points on the curves of a single line style in Fig. 3. Assuming uncorrelated gaussian errors in the three redshifts z_i implies total uncertainties of

$$\Delta\Omega_0 = \sqrt{\sum_i (\partial\Omega_0/\partial z_i \ \Delta z_i)^2}$$

$$\Delta\lambda_0 = \sqrt{\sum_i (\partial\lambda_0/\partial z_i \ \Delta z_i)^2} \qquad (5)$$

where $i = 0, 1, 2$.

Any set of four (idealised) topological images forming *tangentially separated* pairs at z_1 and z_2 as in Fig. 1 would similarly correspond to a combination of two points on the curves of a
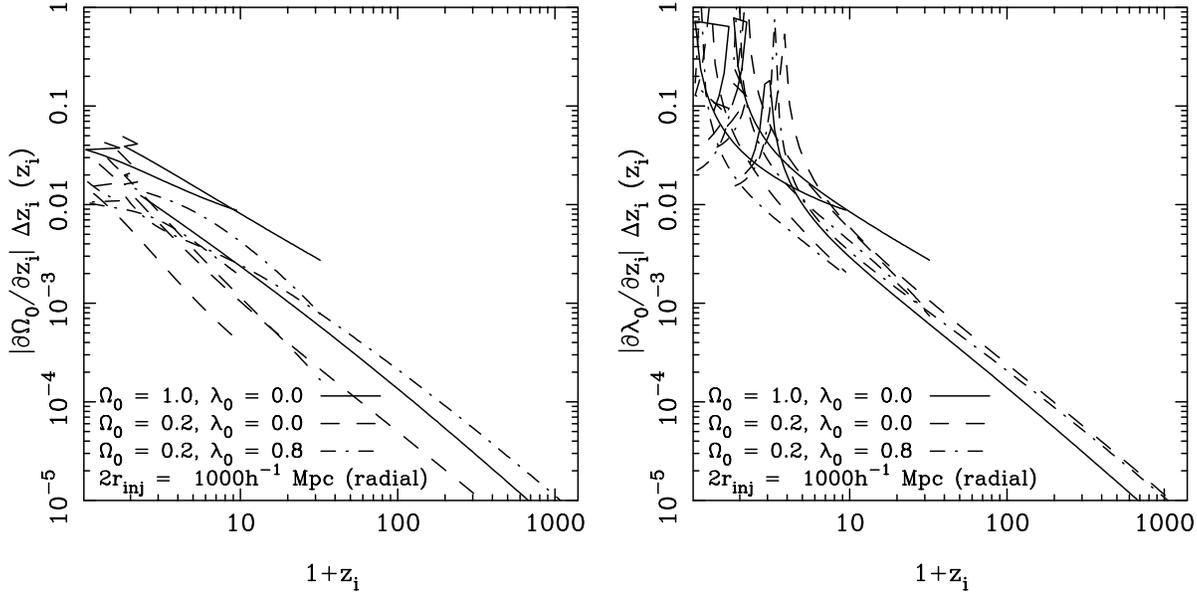
Fig. 3. Radial dependence of uncertainty in Ω_0 (left) and λ_0 (right) on redshifts of topological images, assuming a cosmological redshift uncertainty of $\Delta z = 0.002$ and $2r_{\rm inj} = 1000h^{-1}$ Mpc. The three curves for each set of curvature parameters are for three topological images at $z_0 < z_1 < z_2$ in a radial direction, such that $d(z_1) - d(z_0) = d(z_2) - d(z_1) = 2r_{\rm inj}$.
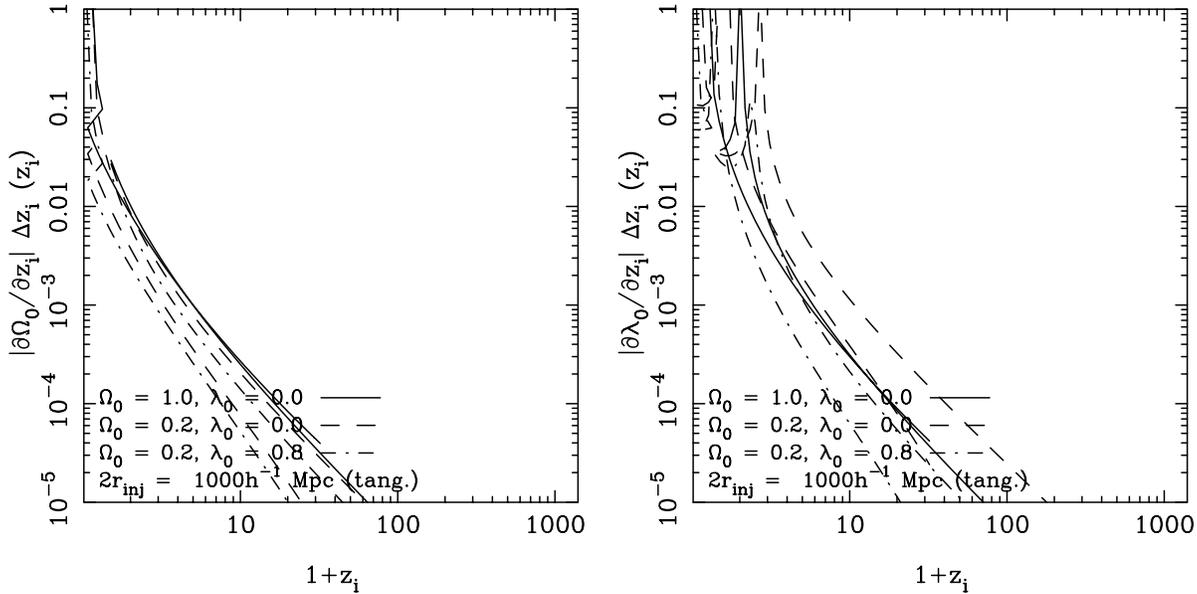
Fig. 4. Tangential dependence of uncertainty in Ω_0 (left) and λ_0 (right) on redshifts of topological images, assuming a cosmological redshift uncertainty of $\Delta z = 0.002$ and $2r_{\rm inj} = 1000h^{-1}$ Mpc. The two curves for each set of curvature parameters are the redshifts $z_1 < z_2$ such that $d(z_2) - d(z_1) = 2r_{\rm inj}$ and that there exists a pair of topological images separated by $2r_{\rm inj}$ along an arc at z_1, and another pair also separated by $2r_{\rm inj}$ at z_2.

single line style in Fig. 4. Eq. (5) would then give the total uncertainties, where $i = 1, 2$.

A real set of topological images would have a less simple set of orientations, so the real uncertainties for a set of three or four objects would consist of interpolations between these two components.

The limiting term in improving the precision of the constraints is clearly the lowest redshift of the triplet or the quadruplet.

Note that $\partial\lambda_0/\partial z_i$ changes sign at a low redshift (the plots show absolute values, so this appears as a cusp). This is simply due to the transition between the regimes where λ_0 has a negligible effect on the metric and where it has a significant effect.

The dependence of λ_0 on changes in z_i changes sign at low redshifts (the plots show absolute values), below which the effect of λ_0 on the radial component of the metric becomes weaker than that of Ω_0.

It should also be noted that the precision of 10^{-6} to 10^{-7} for images at $z \sim 1000$ (off the scale of the figures as shown) is not of practical significance for known astrophysical objects, though if a generation of $\sim 10^6 M_\odot$ collapsed objects containing population III stars existed following the recombination epoch, their eventual detection is not totally impossible.

The precision of 10^{-6} to 10^{-7} at the SLS itself would only be valid if sub-SLS objects were identified with CMB features, and if the redshift of the features in the CMB were precise to $\Delta z = 0.002$. If a more realistic figure of $\Delta z \sim 100$ (as mentioned above) is used for the CMB 'spots', then the uncertainty in Ω_0 and λ_0 is a factor of 5×10^4 times higher than shown in the figures, i.e. the precision is about the same order of magnitude as that possible from sub-SLS objects.

3.2. Simulations

Simulations as described in Sect. 2.2.4 were performed for the popular values of $\Omega_0 = 0.3, \lambda_0 = 1 - \Omega_0$, supposing that successive observations reveal cluster images at the positions predicted from the Roukema & Edge (1997) $T^2 \times R$ candidate in the order illustrated in Fig. 2. Since the density parameter is low in this model, the birth of the cluster can be at a quite high redshift (though this also depends on other parameters like the slope of the primordial power spectrum).

Table 1 shows the resulting uncertainties in the value of Ω_0. As expected, accuracies greater than 1% can easily be obtained from a dozen images with $z \lesssim 3$.

4. Discussion

The calculations presented show the precision obtained if only a few topological images have been reliably identified. However, once this has been done, further multiple topological images of the same object and multiple topological images of other objects will be easier to find. This should yield preciser values still of both the curvature parameters and the generators, so the finding of new corresponding topological images would increase exponentially until saturated by the limits of observational catalogues.

The improvement in accuracy can be estimated as follows.

We can consider a set of four objects at relative positions, neither aligned radially nor tangentially, as providing *both* the radial and tangential separation components as presented above. In that case, if there are a total of N multiple topological images of a single object (e.g. the brightest X-ray cluster known), these can be considered as $N/4$ independent sets of four images. Label the maximum uncertainties for any such set of four images as $\Delta(\Omega_0, 4)$ and $\Delta(\lambda_0, 4)$.

Label the number of physically distinct objects, for which each has about N multiple topological images identified, as M.

Table 1. Uncertainty in estimation of Ω_0 for a simulation based on a candidate 3-manifold which is (hypothetically) confirmed by successive observations of cluster images at predicted positions $i = 4, ..., 12$. Uncertainties of $\Delta z = 0.002$ in the use of redshift as a cosmological distance indicator are used to randomly perturb the positions. The 'best estimate' of the value of Ω_0 is then deduced from the perturbed values. The input value used is $\Omega_0 = 0.3$. The model is flat, so $\lambda_0 \equiv 1 - \Omega_0$. As a function of the total number, i_{max}, of topological images identified, according to the scheme in Fig. 2, the highest redshift of those objects z and the mean and standard deviation of the deduced values of Ω_0 ($\langle \Omega_0 \rangle$, $\Delta \langle \Omega_0 \rangle$ respectively) are listed here.

i_{max}	z	$\langle \Omega_0 \rangle$	$\Delta \Omega_0$
5	0.45	0.2981	12.1×10^{-3}
6	0.69	0.3003	5.4×10^{-3}
7	1.01	0.3002	2.6×10^{-3}
8	1.23	0.3003	2.2×10^{-3}
9	1.85	0.3002	1.5×10^{-3}
10	2.11	0.3001	1.3×10^{-3}
11	3.24	0.3002	1.2×10^{-3}
12	3.63	0.3000	1.2×10^{-3}

Then, the independence of gaussian errors implies a reduction in the uncertainties:

$$\Delta(\Omega_0, MN) \sim \Delta(\Omega_0, 4)/\sqrt{MN/4}$$
$$\Delta(\lambda_0, MN) \sim \Delta(\lambda_0, 4)/\sqrt{MN/4}. \qquad (6)$$

The total number of galaxies visible to apparent magnitude limits of $V \sim 26$ is $MN \sim 10^{10}$–10^{11}. So, if $2r_{inj}$ is small enough that the majority of galaxies have at least four multiple images at epochs later than the galaxies' formation epoch, then the ultimate precision in estimating the curvature parameters could reach around 10^{-6}–10^{-7}, once all-sky redshift surveys with spectroscopy to a precision better than $\Delta z \sim 0.001$ and complete to $V \sim 26$ are performed. This is not attainable in the coming decade, but could be envisaged as a project for the New Generation Space Telescope (NGST).

5. Conclusions

If our Universe corresponds to a Friedmann-Lemaître model, and if the hypothesis of a trivial topology is observably wrong, then the detection of multiple topological images would enable constraints on the curvature parameters from known astrophysical objects to be made as precisely as those presently expected for the Planck and MAP satellites.

The dependence of the precision on the redshifts of the multiple topological images and on their radial and tangential separations has been presented and calculated.

The tangential separations give tighter constraints than the radial separations. Sets of multiple topological images at redshifts $z \lesssim 3$ would imply values of Ω_0 and λ_0 preciser than $\sim 1\%$ and $\sim 10\%$ respectively. The precision available from the Planck and MAP satellites for CMB 'objects' cross-identified with low redshift objects would be similar.

Looking further into the future, an all sky spectroscopic survey by the NGST could lead to precision on a scale impressive by today's standards: 10^{-6}–10^{-7}. Observational cosmology would shift from the phase of working out the basics to that of high precision science.

References

Arnaud M., 1996, J. A. F.52, 26

Bernshtein I.N., Shvartsman V.F., 1980, Sov.Phys.JETP52, 814

Bond J.R., 1996, In: Schaeffer R., Silk J., Spiro M., Zinn-Justin J. (eds.) Cosmologie et structure à grande échelle. Elsevier, Amsterdam, p. 475

Bond J.R., Pogosyan D., Souradeep T., 1998, Class. Quant. Grav.15, 2573 (astro-ph/9804041)

Carlip S., 1998, Class. Quant. Grav.15, 2629 (gr-qc/9710114)

Cayón L., Smoot G., 1995, ApJ452, 487

Chiba M., Yoshii Y., 1997, ApJ489, 485

Cornish N.J., Spergel D.N., Starkman G.D., 1996, Phys.Rev.Lett.77, 215

Cornish N.J., Spergel D.N., Starkman G.D., 1998a, Phys.Rev.D57, 5982 (astro-ph/9708225)

Cornish N.J., Spergel D.N., Starkman G.D., 1998b, Class. Quant. Grav.15, 2657 (astro-ph/9801212)

de Sitter W., 1917, MNRAS78, 3

Dowker H.F., Garcia R.S., 1998, Class. Quant. Grav.15, 1859 (gr-qc/9711042)

Dowker H.F., Surya S., 1998, PhysRevD58, 124019 (gr-qc/9711070)

e Costa S.S., Fagundes H.V., 1998, gr-qc/9801066

Fagundes H.V., 1996, ApJ470, 43

Fagundes H.V., Wichoski U.F., 1987, ApJ322, L5

Fort B., Mellier Y., Dantel-Fort M., 1997, A&A321, 353

Friedmann A., 1924, Zeitschr.für Phys.21, 326

Fukugita M., Yamashita K., Takahara F., Yoshii Y., 1990, ApJ361, L1

Gurzadyan V.G., Torres S., 1997, A&A321, 19

Ionicioiu R., 1998, gr-qc/9711069

Lachièze-Rey M., Luminet J.-P., 1995, Phys. Rep.254, 136

Lehoucq R., Luminet J.-P., Lachièze-Rey M., 1996, A&A313, 339

Lehoucq R., Luminet J.-P., Uzan J.-Ph., 1999, A&A, 344, 735 (astro-ph/9811107)

Lemaître G., 1958, in Stoops R. (ed.) La Structure et l'Evolution de l'Univers. Onzième Conseil de Physique Solvay, Stoops, Brussels, p. 1

Levin J., Scannapieco E., Silk J., 1998, Class. Quant. Grav.15, 2689

Linde A., 1996, astro-ph/9610077

Loveday J., 1998, In: Thuan T.X., et al. (eds.) Dwarf Galaxies and Cosmology. Editions Frontières, Gif-sur-Yvette, France, in press (astro-ph/9605028)

Luminet J.-P., 1998, gr-qc/9804006

Luminet J.-P., Roukema B.F., 1999, astro-ph/9901364

Madore J., Saeger L.A., 1998, Class. Quant. Grav.15, 811 (gr-qc/9708053)

Miralles J.M., Pelló R., Roukema B.F., 1999, submitted

Mostow G.D., 1973, Ann.Math.Studies 78, Princeton University Press, Princeton, USA

Peebles P.J.E., 1993, Principles of Physical Cosmology. Princeton Univ. Press, Princeton, USA

Perlmutter S., Aldering G., Goldhaber G., et al., 1999, astro-ph/9812133

Prasad G., 1973, Invent.Math.21, 255

Rosales J.-L., 1998, gr-qc/9712059

Roukema B.F., 1996, MNRAS283, 1147

Roukema B.F., 1999, MNRAS, submitted

Roukema B.F., Bajtlik, S., 1999, MNRASin press, (astro-ph/9903038)

Roukema B.F., Blanloeil V., 1998, Class. Quant. Grav.15, 2645 (astro-ph/9802083)

Roukema B.F., Edge A.C., 1997, MNRAS292, 105

Schwarzschild K., 1900, Vier.d.Astr.Gess.35, 337; English translation is: Schwarzschild K., 1998, Class. Quant. Grav.15, 2539

Starkman G.D., 1998, Class. Quant. Grav.15, 2529

Stevens D., Scott D., Silk J., 1993, Phys.Rev.Lett.71, 20

Weeks J.R., 1998, Class. Quant. Grav.15, 2599 (astro-ph/9802012)

Weinberg S., 1972, Gravitation and Cosmology. Wiley, New York

White M., Scott D., Silk J., 1994, ARA&A32, 319

Uzan J.-Ph., Lehoucq R., Luminet J.-P., 1999, A&A, in press (astro-ph/9903155)